https://doi.org/10.1016/j.snb.2018.10.164

Use of Carbon Supports with Copper Ion as a Highly Sensitive Non-Enzymatic Glucose Sensor

*Weiran Zheng, Yong Li, Liangsheng Hu, and Lawrence Yoon Suk Lee**

Department of Applied Biology and Chemical Technology and the State Key Laboratory of Chemical Biology and Drug Discovery, The Hong Kong Polytechnic University, Hung Hom, Kowloon, Hong Kong SAR, China.

*lawrence.ys.lee@polyu.edu.hk (L. Y. S. Lee)

KEYWORDS: glucose sensor, copper ion, graphite, activated carbon, carbon paper, MWCNT

Abstract: Nearly all current non-enzymatic electrochemical glucose sensors involve carefully designed metal/metal oxide nanomaterials and the complications of preparing electrocatalyst increase the fabrication cost and reduce the reproducibility of a sensor. Thus, a simple yet reliable and cost-effective glucose sensing system is much desired. Inspired by the glucose oxidation mechanism of copper-based nanomaterials, we developed a series of highly sensitive electrochemical glucose sensors using micromol level Cu^{2+} ions as an electrocatalyst. High sensitivities are achieved on various carbon-based electrodes (GCE: 614 mA M^{-1} cm^{-2}; activated carbon: 1,627 mA M^{-1} cm^{-2}; carbon paper: 2,149 mA M^{-1} cm^{-2}; graphite powder: 1,695 mA M^{-1} cm^{-2}, and functionalized multi-walled carbon nanotube: 1,842 mA M^{-1} cm^{-2}). With short response time (<2 s), large linear range (0.02 μM ~ 2.5 mM and 2.5 ~ 8.0 mM), high stability, and excellent tolerance to interference, Cu ion-based sensor was also validated for testing glucose level in real blood samples. Further studies show that carbon support (*e.g.*, MWCNT-COOH) can be doped with nanomolar level Cu^{2+} to produce a practical solid electrode with an ultra-high sensitivity of 1,732 mA M^{-1} cm^{-2}, retaining the advantage of atomic efficiency. This work provides a new route to the rational design of simple, cheap, and highly effective electrochemical glucose sensors.

1. Introduction

Glucose electrooxidation is an important reaction involved in many research areas including fuel cell,[1, 2] biosensor,[3] and biomass conversion.[4] Especially, glucose sensor development is of vital importance regarding environmental monitoring and medical diagnosis.[5] The World Health Organization reported a total number of 422 million adults with diabetes in 2014 and 1.5 million death caused by diabetes in 2012 alone.[6] Moreover, diabetes prevalence has been rising steadily and rapidly in the middle- and low-income countries. Thus, the need for developing a cheap, stable, and efficient glucose sensing system is of critical urgency.

Since the first enzyme-based glucose biosensor was reported decades ago, two types of glucose sensors have been developed to date: enzyme-based and non-enzyme-based.[7, 8] Despite high selectivity, enzyme-based glucose sensors suffer from high cost and low stability. Such disadvantages, mainly associated with the use of an enzyme, have led to the development of non-enzymatic glucose sensors, mostly metal-containing electrocatalysts (Ni,[9] Co,[10] Cu,[11-14] Pt,[15], *etc.*) of various morphologies. In particular, copper-based nanomaterials (Cu,[11] CuO,[12] Cu_2O,[13] $Cu(OH)_2$,[14], *etc.*) are considered as the most promising catalysts due to their high activity and low cost. Most of the efforts have been made to expose more active sites and increase the conductivity, such as optimising the catalyst support (carbon nanotube,[16], C_3N_4,[17] graphene,[18, 19] conductive polymer,[11], *etc.*) and altering the morphology.[20] Although the sensitivity towards glucose has been largely improved, similar problems persist, such as long-term stability and surface poisoning.[21] Moreover, the use of sophisticated nanostructures inevitably raises the fabrication cost, which contradicts the original intention of designing a cheap glucose sensing system.

From catalysis perspective, nearly all copper-based glucose sensors engage electrochemically produced surface Cu(III) species as the active sites for glucose electrooxidation.[22, 23]

Majority of Cu atoms in bulk nanostructures, however, would not directly interact with glucose. Very recently, we reported that Cu^{2+} ions could act as an efficient electrocatalyst for glucose oxidation.[24] By forming a Cu(II)-glucose complex in alkaline solution, Cu(II) species effectively transfer the electron from the electrode to glucose within the double layer region, which dramatically lowers the overpotential of glucose oxidation. Such an unexpected high catalytic activity of Cu(II) species leads us to design a new type of glucose sensor based on Cu ions, without involving solid-state nanostructures. With every Cu atom engaged as an active catalytic site, the maximum atomic efficiency, thus better sensitivity, is anticipated.

Herein, we investigated different types of carbon electrodes (glassy carbon electrode (GCE), activated carbon, conductive carbon paper, graphite powder, and functionalized multi-walled carbon nanotube (MWCNT-COOH)) to design a glucose sensor based on homogenous Cu^{2+} ions (μM level). With optimised potential and Cu^{2+} concentration, excellent sensitivities were achieved. Moreover, an example of practical sensor design is given by localizing Cu^{2+} ions (nM level) on a functionalized MWCNT-modified GCE, which retains the high sensitivity and demonstrates its potential application in real life as a solid electrode. The common aspects of sensors, such as stability, response time, and interference studies, are carried out as well.

2. Experimental

2.1. Material

Activated carbon (Darco, Sigma-Aldrich), graphite powder (Union Carbide, <1ppm impurities), conductive carbon paper (HCP030N, Chuxi, Shanghai, 3mΩ cm^{-2}), carboxylic acid-functionalized carbon nanotube (Multi-walled, Timesnano, China), Nafion-perfluorinated ion-exchange resin (Sigma-Aldrich), sodium hydroxide (>96%, Uni-chem), D-(+)-glucose (>99.5%, Sigma-Aldrich), and copper(II) nitrate (Sigma-Aldrich) were used as received. All aqueous solutions were prepared using double-deionised water (DI water) from MilliQ Water System (Millipore, USA, R>18.2 MΩ cm^{-1}).

2.2. Electrode preparation

Glassy carbon electrode (GCE, 3 mm diameter, surface area = 0.071 cm^2) was polished with 1.0, 0.3, and 0.05 μm α-Al_2O_3 powders (CH Instruments) before use. The electrode was rinsed with DI water and acetone. The cleaned electrode was dried at room temperature before surface modification.

To prepare modified GCE, Nafion-activated carbon ink (1 mg mL^{-1}, Nafion: 0.25 wt%), carboxylic acid functionalized carbon nanotube (MWCNT-COOH) ink (1 mg mL^{-1}), and graphite powder ink (1 mg mL^{-1}, Nafion: 0.25 wt%) in DI water was drop cast on the GCE surface and air-dried at room temperature for 2 h. The volumes of as-prepared inks used were varied to achieve various areal capacity.

Carbon paper was cut to a specific geometric size and directly used as a working electrode with an electrode holder after washing with acetone and DI water.

2.3. Cu(II)-localized MWCNT-COOH electrode preparation (Cu(II)/MWCNT-COOH)

MWCNT-COOH was dispersed in DI water (10 mg mL^{-1}), and the suspension was sonicated for 30 min, followed by the addition of Cu^{2+} aqueous solution with various Cu to MWCNT-COOH mass ratio (1:100 to 1:2). The mixture was sonicated for another 30 min, and 10 μL mixture ink was drop cast on the GCE surface and air-dried at room temperature for 2 h.

2.4. Apparatus

Cyclic voltammetry (CV) and amperometric *i*-t electrochemical measurements were performed on a CHI 1030A electrochemical analyser (CH Instruments, Inc., USA). A three-electrode system was adopted for all electrochemical measurements. Saturated calomel electrode (SCE) and Pt wire were used as the reference and counter electrode, respectively, with the scan rate of 5 mV s^{-1}. For all experiments, 10 mL of 0.1 M NaOH was used as the electrolyte with continuous stirring at 1,070 rpm. For the *i*-t tests, the electrode was first stripped for 10 cycles

between 0 and 1 V (*vs.* SCE, unless stated otherwise) to clean the surface. Various amounts of $Cu(NO_3)_2$ solution (100 mM) were added to the electrolyte, 50s after the target potential was applied. Starting from 1,000s, glucose solution was added every 50s with stirring at 1,070 rpm. The geometric area of GCE and carbon paper was used to calculate the sensitivity values of modified GCE and carbon paper electrodes. The sensitivity values with error bar were evaluated based on five repeated experiments. Electrochemical impedance spectroscopic (EIS) measurements were conducted on a PARSTAT 2273 electrochemical system (Princeton Applied Research) from 1 MHz to 10 mHz at 0.60 V. The areal capacities of modified GCE electrodes and carbon paper were measured by cycling the potential between 0.15 and 0.20 V with different scan rates (5, 10, 15, 20, and 25 mV s^{-1}). Transmission electron microscopy (TEM) images were obtained from a JEOL TEM instrument (Model JEM-2100F). X-ray diffraction (XRD) was performed on X'Pert PRO PHILIPS with Cu Ka radiation, and Raman scattering spectroscopy was carried out by Renishaw inVia Micro-Raman Spectroscopy System. The chemical states of materials were determined by X-ray photoelectron spectroscopy (XPS, AC-2, Riken Keiki), and GL(30) line profile was used for peak fitting. High-performance liquid chromatography (HPLC) was provided by Agilent Technologies (1200 Series) with a refractive index detector (RID). The column used in ambient condition was Prevail Carbohydrate ES 5 μm (250 mm × 4.6 mm) by Grace. A mixture of acetonitrile (75%) and water (25%) was used as mobile phase at a flow rate of 0.7 mL min^{-1}. The serum samples were injected to HPLC-RID after filtration and centrifugation. The surface area analysis was done on a Micromeritics ASAP 2020 Plus Physisorption analyser using N_2.

3. Results and Discussion

3.1. CV study of Cu(II) and glucose in alkaline solution

In alkaline solutions, Cu^{2+} ions coordinate with OH^-, forming $Cu(OH)_2$, $Cu(OH)_3^-$, and $Cu(OH)_4^{2-}$.[25] In 0.1 M NaOH aqueous solution (pH=13), the dominant species is $Cu(OH)_3^-$

(or $HCuO_2^-$). For clarification, all species containing Cu^{2+} are labelled as Cu(II), and the Cu(II) concentration refers to the total concentration of all Cu^{2+} species.

Figure 1a shows the CV plots of bare GCE in an electrolyte containing both Cu(II) and glucose. After adding glucose, a dramatic rise in oxidation current appears from 0.35 V, while no such signal is observed for only glucose nor Cu(II). It shows that Cu(II) can act as an electrocatalyst for glucose oxidation, efficiently decreasing the oxidation potential of glucose on GCE. The catalytic reaction mechanism of Cu ion has been previously reported.[24] Based on the highly efficient catalytic activity of Cu(II), we report herein an electrochemical system for glucose sensing.

3.2. Cu(II)–based glucose sensing system: a proof of concept

Figure 1b illustrates a proof-of-concept procedure of Cu(II)-catalyzed glucose sensing system. For amperometric response tests, a three-electrode system was used under continuous stirring. A target potential was applied until the background current stabilized. In a typical sensing experiment, the Cu(II) ions are added at 50s, which causes an instant current rise. The electrochemical reactions associated with this signal (reaction 1 and 2) are illustrated in **Figure 1c**: Cu(II) species are oxidized to Cu(III), which is rapidly reduced by water, producing $Cu(OH)_2$ and O_2.[26]

$$Cu(II) \rightarrow Cu(III) + e^- \quad (1)$$

$$Cu(III) + 4OH^- \rightarrow Cu(II) + 2H_2O + O_2 \quad (2)$$

Upon the addition of glucose at 1,000s, another instant current signal is observed. This current is associated with the electrooxidation of Cu(II)-glucose complex as shown in **Figure 1d**: Cu(II) species coordinated with glucose (Cu(II)-glucose) is oxidized to Cu(III)-glucose on the electrode surface. Such Cu(III)-glucose complex is not stable and would go through the self-redox process, producing gluconolactone and Cu(II) (reaction 3 and 4).[24]

$$Cu(II)\text{-glucose} \dashrightarrow Cu(III)\text{-glucose} + e^- \quad (3)$$

$$\text{Cu(III)-glucose} \rightarrow \text{gluconolactone} + \text{Cu(II)} \quad (4)$$

As a proof of concept model, bare GCE was used in 0.1 M NaOH solution. **Figure 2a** shows the amperometric response of bare GCE to glucose in the presence of different concentration of Cu(II) at various applied potentials. An immediate current increase is observed after Cu(II) injection, which stabilizes after 400s. This process is related to the establishment of double layer species as shown in **Figure 1c**. At 1,000s mark, the addition of glucose causes a significant and instant current response. The response signal rises according to the glucose concentration added, and the reaction equilibrium is quickly reached within 2s **(Figure 1d)**. Based on the *i*-t plots, the corresponding sensitivity was calculated for various Cu(II) concentration and potentials conditions **(Figure 2b)**. At a given applied potential, different optimal Cu(II) concentrations to reach the highest sensitivity are noted: 445, 523, and 614 mA M^{-1} cm^{-2} with 0.1 mM Cu(II) at 580 mV, 0.15 mM Cu(II) at 590 mV, and 1.0 mM Cu(II) at 600 mV. The optimal Cu(II) concentrations with applied potential at 610 mV and 620 mV are higher than 2 mM. As shown, the highest sensitivity of GCE towards glucose was obtained with 1 mM Cu(II) at the applied potential of 600 mV. Surprisingly, such a simple and unmodified system shows the high sensitivity that is comparable to those reported in the literature. For instance, well-designed CuO nanomaterials have a sensitivity of ~400 mA M^{-1} cm^{-2} towards glucose.[27, 28]

3.3. Using carbon-based materials as electrode

The simple GCE-Cu(II) system shows a promising sensitivity. However, GCE is never an ideal electrode for sensor design due to its limited surface area (0.071 cm^2 in our experiments). We have therefore investigated other carbon-based electrodes for enhanced glucose sensing. Based on the different aspects (surface area, conductivity, and surface properties), we selected activated carbon, carbon paper, graphite powder, and carboxylic acid-functionalized multi-walled carbon nanotube (MWCNT-COOH) to demonstrate the universality of Cu(II)–based

glucose sensing system. Activated carbon is a porous material with high surface area, which can provide more binding sites for Cu(II) ions. Carbon paper is a three-dimensional network of carbon fibers with a high surface area and conductivity. Graphite has a unique layered structure with outstanding electron transfer ability. MWCNT-COOH offers high conductivity and surface area. Also, the –COOH groups on its outer wall provide anchor points for Cu(II).[29]

Figure 3(a-d) shows the CV plots of aforementioned carbon-based electrodes in 0.1 M NaOH solution containing 1 mM Cu(II), 5 mM glucose, and 1 mM Cu(II) with 5 mM glucose. Only in the presence of Cu(II), all carbon-based materials show electrooxidation current between 0.4 and 0.7 V, which suggests that Cu(II) is the electrocatalyst for glucose electrooxidation. Interestingly, when activated carbon and graphite powder were used as electrocatalyst support (**Figure 3a** and **3c**), a broad oxidation peak (0.40 V ~ 0.70 V) is evident, while no current peaks are found using carbon paper (**Figure 3b**). Such a difference could be due to the different routes of mass transfer of Cu(II)-glucose caused by the structural difference of carbon supports. However, for MWCNT-COOH, in the presence of Cu(II) in the electrolyte, two oxidation peaks are observed at 0.40 and 0.75 V (**Figure 3d**). Such two redox processes were not observed with other Cu[30] or Cu_2O[31] systems involving MWCNT. The evolution of current peaks is not only controlled by the electron transfer rate of active sites but also the mass transfer of Cu(II)-glucose. In this case, those peaks could be caused by the different mass transfer route to various binding sites of MWCNT-COOH for glucose oxidation, such as tube defects and edges. **Figures 3(e-h)** summarise the sensitivity values of carbon-based electrodes toward glucose detection using various Cu(II) concentrations. The initial increase of Cu(II) concentration from 5 to 100 μM leads to the sensitivity enhancements for all types of carbon-based electrodes. The sensitivities, however, reach a plateau (or a slight drop) after a certain Cu(II) level. Each carbon-based electrode requires different Cu(II) concentrations for the

highest sensitivity: 0.1 mM on activated carbon (25 µg) modified GCE (1,021 mA M^{-1} cm^{-2}), 0.2 mM on carbon paper (2,149 mA M^{-1} cm^{-2}), 1 mM on graphite powder (15 µg) modified GCE (1,695 mA M^{-1} cm^{-2}), and 0.1 mM on MWCNT-COOH (10 µg) modified GCE (1,842 mA M^{-1} cm^{-2}). These sensitivities are among the highest values reported to date (**Table 1**).

The sensitivity enhancements observed from four electrodes can be attributed to the increased number of binding sites for Cu(II), which results in more electrons transfer between carbon and Cu(II), producing more Cu(III). Thus, more glucose molecules are oxidized during the same period, *i.e.*, higher current. Once the electrochemical surface of the electrode is saturated, further increase in Cu(II) concentration does not enhance the sensitivity.

Figure 3i shows the N_2 adsorption-desorption isotherms plots of carbon-based materials and the Brunauer–Emmett–Teller (BET) surface area was calculated to be 217.7 m^2 g^{-1} for activated carbon, 318.8 m^2 g^{-1} for MWCNT-COOH, 45.7 m^2 g^{-1} for carbon paper, and 29.3 m^2 g^{-1} for graphite powder. It shows that activated carbon and MWCNT-COOH have much larger surface areas than carbon paper and graphite powder. To study the effect of surface area, the activated carbon mass applied on the GCE surface was changed (25, 50, and 100 µg) and tested for the sensitivity. **Figure 3e** shows that the sensitivity increases with the mass of activated carbon on GCE and reaches the highest values of 1,021, 1,317, and 1,627 mA M^{-1} cm^{-2}, respectively. These sensitivity values correlate well with the calculated areal capacities of activated carbon on GCE (11.4, 15.8, and 30.0 mF cm^{-2}), confirming that a larger electrochemical surface area provides more Cu(II) binding sites, which can promote the sensitivity of electrodes towards glucose detection.

Table 1. Comparison of our results with the state-of-the-art copper-based non-enzymatic glucose sensors on modified GCE.

Electrocatalyst	Sensitivity (mA M^{-1} cm^{-2})	Linear range (mM)	Detection limit (µM)	Ref.
CuO nanosphere	404	0.001 - 2.55	1	[28]
CuO nanofibers	431	0.006 - 2.5	0.8	[32]

Cu nanowires	420	0.0001 - 3	0.035	[33]
Cu/polyaniline/graphene	150	0.003 – 3.7	0.27	[11]
CuO flowers/graphite	709	0.004 - 2	4	[27]
Cu nanoparticles/graphene oxide/SWCNT	930	0.001 - 4.5	0.34	[34]
CuO nanoparticle/graphene	1,065	0.001 - 8	1	[35]
CuO/SWCNT	1,610	0.0001 - 1.8	0.05	[36]
Cu nanoparticles/pencil graphite	1,467	0.1 - 1	0.44	[37]
Candy like CuO	1,729	0.5 – 5.0	0.9	[38]
CuO nanowire/SWCNT	761.5	0.001 – 2.67	0.0456	[39]
activated carbon (100 µg) + Cu(II) (1 mM)	1,627	0.0004 - 7	0.2	this work
graphite powder (15 µg) + Cu(II) (1 mM)	1,695	0.00007 - 5	0.05	this work
MWCNT-COOH (10 µg) + Cu(II) (100 µM)	1,842	0.00002 – 2.5 & 2.5 – 8	0.02	this work
Cu(II)/MWCNT-COOH (1:5) (*i.e.*, Cu(II)=31 nmol)	1,732	0.0003 – 9	0.3	this work

For comparison, the sensitivity values are normalized by plotting against the measured areal capacity of carbon-based materials (**Figure 3j**). The weight of carbon materials (activated carbon, graphite powder, and MWCNT-COOH) coating on GCE and the geometric area of carbon paper was tuned to achieve different areal capacities. The Cu(II) concentration is fixed at 1 mM to make sure that the electrode surfaces are saturated and the highest sensitivity can be obtained. As shown in **Figure 3j**, the sensitivities show a linear correlation towards the areal capacity of the carbon materials. The fitted slope indicates the nature of electrodes; graphite shows the highest sensitivity (4,151 mA M^{-1} mF^{-1}), followed by carbon paper (258.0 mA M^{-1} mF^{-1}), MWCNT-COOH (244.4 mA M^{-1} mF^{-1}), and activated carbon (62.9 mA M^{-1} mF^{-1}). Although graphite powder shows the highest slope value, it is practically difficult to increase its areal capacity due to the instability of coating layer. For 20 µg graphite powder loading, a small surface capacity of 0.226 mF cm^{-2} is obtained. The use of carbon paper shares the similar problem that it requires large geometrical size for high areal capacity. The activated carbon shows a very high areal capacity (15.8 mF cm^{-2} for 50 µg activated carbon/GCE), but the sensitivity gain is not as high as other carbon electrodes, as the gentle slope suggests the

inefficient electron transfer between carbon and Cu(II) species. It is also worthwhile to note that the sensitivity does not further increase at high areal capacity for the case of MWCNT-COOH, due to the mass transfer limit of glucose.

The electrochemical impedance spectroscopic (EIS) measurements are carried out to compare the conductivity of four materials. A fixed potential of 0.60 V is applied to all electrodes with a perturbation amplitude of 5 mV RMS (root mean square). Four electrochemical electrolytes were tested, including i. 0.1 M NaOH; ii. 0.1 M NaOH containing 1 mM Cu(II); iii. 0.1 M NaOH containing 5 mM glucose; and iv. 0.1 M NaOH containing 1 mM Cu(II) and 5 mM glucose. The Nyquist plots are fitted with a simplified Randles cell and presented in **Figure 4**. In 0.1 M NaOH solution, the fitted resistance of charge transfer (R_{ct}) reflects the difficulty of OH^- adsorption/oxidation/desorption on carbon material. Graphite powder shows the highest resistance (22.9 kΩ), followed by MWCNT-COOH (2.2 kΩ), activated carbon (1.9 kΩ), and carbon paper (1.7 kΩ). When Cu(II) or glucose are added to the electrolyte, the resistance decreases for all electrodes, suggesting that both Cu(II) adsorption/oxidation/desorption and glucose adsorption/desorption are faster than OH^- adsorption/desorption process. With both Cu(II) and glucose present, the smallest resistance values are observed. Such dramatic decrement in the resistance indicates that the surface reaction between Cu(II) oxidation and glucose oxidation occurs *via* a shortcut pathway.[24] Carbon paper shows the lowest charge transfer resistance (48.0 Ω), followed by graphite (67.6 Ω) and MWCNT-COOH (269.6 Ω). The highest resistance of 613.5 Ω is observed on activated carbon/GCE. Both surface property and conductivity differences of carbon materials lead to such resistance difference. Taking the surface area **(Figure 3i)**, sensitivity gain **(Figure 3j)**, and resistance **(Figure 4)** factors into consideration, MWCNT-COOH seems to be the most suitable carbon support.

3.4. Interference, stability, linear range, detection limit, and mice blood sample test

In addition to the sensitivity, the selectivity, stability, linear range, and detection limit are also critical parameters for evaluating a sensor. With 0.05 mM Cu(II) present, we have carried out the interference tests using (1) ascorbic acid, (2) dopamine, (3) lactose, (4) sucrose, (5) uric acid, and (6) L-phenylalanine as interferents (**Figure 5a**) at 0.60 V. The Cu(II) was introduced at 50s, and the interferents (10% of the glucose concentration) were added from 1,000s. The average concentration range of the interferents is 0 ~ 5 % that of glucose that is normally above 3.5 mM.[40] The current responses to all the interfering species are trivial compared with that due to glucose, which demonstrates that the Cu(II) ion system has a high selectivity towards glucose. The stability of the system was tested by measuring the current response for an extended period (5,500s, **Figure 5b**). No significant loss of current indicates the excellent stability of such homogeneous catalytic system. **Figure 5c** shows the correlation between glucose concentration and current density using a MWCNT-COOH modified GCE with 0.05 mM Cu(II). Similar to the previous report, two linear ranges[11] were evident: 0.02 μM~2.5 mM and 2.5~8.0 mM. Because Cu-based glucose sensors usually use diluted blood samples, the 0.02 μM~2.5 mM range is applicable for glucose detection. In this range, such a sensor shows a sensitivity of 1,180 mA M^{-1} cm^{-2} and a coefficient of determination (R^2) of 0.993. With a signal to noise ratio of 3 (S/N = 3), the limit of detection (LOD) is calculated to be 0.02 μM.

A real sample test using mice serum was carried out, and the MWCNT-COOH modified GCE was used for the determination of glucose in mice serum samples at the presence of Cu(II). With an applied potential of 0.60 V on MWCNT-COOH (10 μg) modified GCE, 0.5 mL of mice serum sample was injected into 10 mL of an electrolyte containing 0.1 M NaOH and 0.05 mM Cu(II) species. The pH value of the electrolyte changes from 12.9 to 12.8. The measured current increment was used to calculate the glucose concentration using the sensitivity data

shown in **Figure 5c**. For each mice serum sample, the *i*-t tests were performed six times and the mean value of serum glucose concentration was calculated.

Meanwhile, the mice serum samples were analysed by high-performance liquid chromatography (HPLC) in parallel for verification. Three mice serum samples were tested and the glucose concentrations determined by HPLC and our sensor are summarised in **Table 2**. Based on six tests (n = 6), a relative standard deviation (RSD) was calculated to be 3.2% for serum-1, 2.5% for serum-2, and 3.7% for serum-3, which demonstrates high accuracy and precision of the Cu(II) ion-based glucose sensing system.

Table 2. Mice serum test comparing HPLC and Cu(II) ion-based glucose sensing results.

Serum sample	HPLC result	Cu(II) ion-based glucose sensing system result	RSD (n = 6)
serum-1	6.2 mM	6.4 mM	3.2%
serum-2	5.7 mM	6.1 mM	2.5%
serum-3	5.1 mM	5.2 mM	3.7%

3.5. Localized Cu(II) ion on MWCNT-COOH: a practical example

So far, nearly all electrochemical glucose sensors are based on solid-state electrocatalysts. Although our Cu(II) system has already shown its potential as a highly efficient glucose sensor, the instability of Cu(II) in electrolyte makes it inconvenient for practical use in real life. To produce a solid-state electrocatalyst while retaining the advantage of using Cu(II) (high atomic efficiency), we have anchored Cu(II) ions to MWCNT-COOH to achieve Cu(II)/MWCNT-COOH hybrid material for glucose sensing. The mass ratio of Cu(II) to MWCNT-COOH in the mixture ink is tuned from 1:100 to 1:2.

Figure 6a shows the TEM images of MWCNT-COOH before and after Cu(II) localization. In both samples, the multi-walled structure of carbon nanotube was observed, suggesting no significant destruction of MWCNT during Cu(II) doping. At a Cu/MWCNT-COOH mass ratio of 100:1, no crystallized structure of CuO nor $Cu(OH)_2$ was evident. Raman spectroscopy is

commonly used to analyze carbon materials. **Figure 6b** reveals the Raman spectra of MWCNT-COOH and Cu(II)/MWCNT-COOH. Pure MWCNT-COOH features two bands: D band (~1,370 cm^{-1}) and G band (~1,600 cm^{-1}), which originates from disorder-induced amorphous carbon (defects, lattice distortion, *etc.*) and graphite structure, respectively.[41] The intensity ratio of the D band to G band is used to estimate the disorder degree of carbon materials. Compared with that of MWCNT-COOH (2.77), the intensity ratio of Cu(II)/MWCNT-COOH hybrid materials are smaller. With the ratio of Cu(II)/MWCNT-COOH increasing, the intensity ratio decreases in general (2.55, 2.13, 1.95, 2.08 for Cu(II)/MWCNT-COOH mass ratio of 1:100, 1:20, 1:5, and 1:2, respectively). It is possible that Cu(II) species interacting with -COOH functional groups or defects reduces the total amount of disordered carbon. The gradual shifting of D band to the lower wavenumber (from 1,370 cm^{-1} to 1,323 cm^{-1}) after Cu(II) localization is also notable. Such D band shifting is commonly related to the change of bonding strength (electronic structure) of disordered sections,[42] which suggests the Cu(II) species have strong electronic interaction with surface defect/functional groups of MWCNT-COOH. XPS is also employed to study the surface properties of Cu(II)/MWCNT-COOH materials. The Cu $2p_{3/2}$ and O 1s XPS spectra of Cu(II)/MWCNT-COOH with 1:100 and 1:2 mass ratio were shown in **Figure 6c**. Two Cu species with binding energies of 933.8 and 932.2 eV were evident in 1:2 sample, which can be assigned to CuO and -COO-Cu (Cu(II) coordinating with -COOH) structures. The majority of Cu(II) species exists in the form of -COO-Cu (83%). No Cu $2p_{3/2}$ signal was found in 1:100 sample due to its low Cu content. Two oxygen species at 533.2 and 531.8 eV assigned to C-O and C=O were found in both samples.[43] At higher Cu contents, more C-O was formed, indicating the formation of more Cu-O- (in -COO-Cu) species. The structural properties of Cu(II)/MWCNT-COOH was examined by XRD, as presented in **Figure 6d**. Apart from the broad peak due to the glass sample holder, the characteristic peak of MWCNT (002) was found

in all samples at 25.7°, and no sign of $Cu(OH)_2$ or CuO was discovered. Based on the above material characterization results, we propose the structure shown in **Figure 6e** as the main Cu(II) species present in Cu(II)/MWCNT-COOH hybrid material. Two coordination sites of Cu(II) bind the carboxylate groups on MWCNT, whereas the others coordinate with OH^- and deprotonated glucose molecules.[17, 24]

The glucose electrooxidation using Cu(II)/MWCNT-COOH was studied, and the results are shown in **Figure 7**. **Figures 7(a-d)** present the CV plots of modified GCE with Cu/MWCNT-COOH mass ratio of 1:100, 1:20, 1:5, and 1:2 in 0.1 M NaOH electrolyte with and without 5 mM glucose. At lower mass ratio (1:100), only an oxidation peak at 0.40 V is evident after glucose addition, while two board peaks are shown with a higher mass ratio of Cu/MWCNT-COOH, which is similar to the CV plots shown in **Figure 3d** using MWCNT-COOH with Cu(II) in the electrolyte. It is believed that the evolution of two oxidation peaks is due to the structural feature of the MWCNT-COOH. It is possible that, at high Cu(II) concentrations, two (or more) binding sites for Cu(II) exist on MWCNT-COOH, such as tube defects and edges. Depending on the structure of binding sites, glucose transport routes to the anchored Cu(II) sites are different and thus show different oxidation peak positions. Such results demonstrate that Cu(II)/MWCNT-COOH can serve as an electrocatalyst for glucose electrooxidation. **Figures 7(e-h)** show the corresponding Nyquist plots of Cu(II)/MWCNT-COOH modified GCE in different electrolytes at an applied potential of 0.60 V. MWCNT-COOH shown no activity towards glucose electrooxidation and a high R_{ct} of 25.2 kΩ was recorded. At 0.60 V, Cu(II)/MWCNT-COOH would be oxidized to Cu(III)/MWCNT-COOH, and the R_{ct} was calculated to be 15.3 kΩ (1:100), 11.1 kΩ (1:20), 10.9 kΩ (1:5), and 11.1 kΩ (1:2). Similar to the finding in **Figure 4**, after introducing glucose, the R_{ct} dropped to 4.9 kΩ (1:100), 3.7 kΩ (1:20), 3.2 kΩ (1:5), and 4.3 kΩ (1:2), showing a favourable reaction path towards glucose electrooxidation. It should be noted that the R_{ct} values of Cu(II)/MWCNT-COOH are higher

than that of homogenous system (**Figure 4**), thus indicating that the homogenous system is more efficient.

Figure 8a shows the *i*-t curves of Cu(II)/MWCNT-COOH electrocatalyst at 0.60 V in the presence of various amount of glucose. A stable baseline was achieved within 70 s, significantly shorter than the non-anchored system (**Figure 2a**). The addition of glucose triggered a rapid current response (<2 s). The calculated sensitivity of Cu(II)/MWCNT-COOH electrocatalyst is summarised in **Figure 8b**. The MWCNT-COOH/GCE (without Cu(II) anchoring) shows a sensitivity of 115.4 mA M^{-1} cm^{-2}, mainly due to the current associated with the formation of double-layer structure. As the mass ratio of Cu(II) to MWCNT-COOH increases from 1:100 to 1:5, the sensitivity increases linearly due to the increased total population of active sites. When the Cu(II)/MWCNT-COOH ratio is higher than 1:5, the amount of added Cu(II) exceeds the number of carboxylate groups on MWCNT. Thus no more Cu(II) ions can be anchored onto MWCNT. The highest sensitivity achieved is 1,732 mA M^{-1} cm^{-2} when Cu(II)/MWCNT-COOH mass ratio is 1:5, which is slightly lower than MWCNT-COOH/GCE in 0.1 mM Cu(II) (1,842 mA M^{-1} cm^{-2}). Such decrease in sensitivity is caused by the limited mass transfer of glucose to the anchored Cu(II), compared to the case of free Cu(II) species.

The interference test result is present in **Figure 8c**. For ascorbic acid, uric acid, and L-phenylalanine, the current influences are negligible. Although dopamine, lactose, and sucrose show immediate current changes, they are relatively smaller than that of glucose. **Figure 8d** shows one of the five correlation plots obtained from the repeated experiments. The linear range was found to be 0.3 μM~9.0 mM. In this range, the sensor shows a sensitivity of 1,642 mA M^{-1} cm^{-2} and a coefficient of determination (R^2) of 0.987. With a signal to noise ratio of 3 (S/N = 3), the LOD is calculated to be 0.3 μM. **Figure 8e** shows the stability test of Cu(II)/MWCNT-COOH (1:5) modified GCE. Upon the addition of 100 μM glucose, an

immediate current density increase was found (from 0.075 to 0.246 mA cm^{-2}). After 8,000s, the current remains stable at 0.217 mA cm^{-2} (11.8% current loss). It suggests that the interaction between MWCNT-COOH and Cu(II) ion is stable during the electrochemical tests without significant loss of anchored Cu(II) ions. The mice serum test was also performed using a Cu(II)/MWCNT-COOH (1:5) modified GCE and cross-checked with HPLC results. The blood glucose concentrations determined by the sensor and HPLC are 6.0 and 6.3 mM, respecitively, with a RSD (n = 6) of 1.7%.

It is worth to note that, only nanomolar levels of Cu(II) are present on the electrode (1.5 nmol of Cu(II) on electrode when the mass ratio of Cu(II) to MWCNT-COOH is 1:100). With this small amount of catalyst loading, ultra-high sensitivity (>1,000 mA M^{-1} cm^{-2}) was achieved, which demonstrates an efficient way to make Cu(II) ion system into a solid and promising glucose sensor with the minimum loss of sensitivity.

4. Conclusions

There are two conclusions based on our studies:

1. We have demonstrated a new way of glucose sensing using copper ion together with a series of carbon-based electrodes. Cyclic voltammetry studies prove that Cu(II) added in the alkaline electrolyte can act as an electrocatalyst and boost the electrooxidation rate of glucose. Such a system is further used for glucose sensor design. By using GCE, a considerably high sensitivity of 614 mA M^{-1} cm^{-2} was obtained. The universality of this catalytic system is shown by changing the supporting carbon electrode. Sensitivity values as high as 1,635 mA M^{-1} cm^{-2} (activated carbon modified GCE), 2,149 mA M^{-1} cm^{-2} (carbon paper), 1,695 mA M^{-1} cm^{-2} (graphite powder modified GCE), and 1,842 mA M^{-1} cm^{-2} (MWCNT-COOH modified GCE) were obtained with only μmol level Cu(II) ions present in the electrolyte. Furthermore, a linear correlation was found between sensitivity and areal capacity of carbon-based electrodes. By

altering the electrochemical surface area of supporting electrode and Cu(II) concentration, the sensitivity can be tuned accordingly. This system shows short response time (<2 s), low detection limit (0.02 μM), large linear range (0.02 μM~2.5 mM and 2.5 mM~8.0 mM), high stability, and excellent tolerance to interference.

2. We have developed a simple method to prepare hybrid material with Cu(II) ions anchored on the surface of MWCNT-COOH for glucose sensing. TEM and XRD results show no existence of CuO or $Cu(OH)_2$ nanostructures, while XPS and Raman results suggest a strong electronic interaction between Cu and -COOH functional group. Studies show that such solid electrode pertains the advantage of high sensitivity and stability of homogeneous Cu(II) system. Ultra-high sensitivity (>1,000 mA M^{-1} cm^{-2}) can be achieved using only nmol level Cu(II) ions, and a broad linear range of 0.3 μM ~9.0 mM is demonstrated.

Our study suggests that the copper ion-based glucose sensing system can provide a new route to the rational design of cost-effective and highly efficient electrochemical glucose sensors without involving metal/metal oxide nanomaterial synthesis.

5. References

[1] V. Oncescu, D. Erickson, Sci. Rep. 3 (2013) 1226-1231.
[2] L. Li, K. Scott, E.H. Yu, J. Power Sources 221 (2013) 1-5.
[3] M.M. Rahman, A.J. Ahammad, J.H. Jin, S.J. Ahn, J.J. Lee, Sensors 10 (2010) 4855-4886.
[4] A. Onda, T. Ochi, K. Kajiyoshi, K. Yanagisawa, Appl. Catal., A 343 (2008) 49-54.
[5] A. Brouzgou, P. Tsiakaras, Top. Catal. 58 (2015) 1311-1327.
[6] Global Report on Diabetes, Geneva: World Health Organization, 2016.
[7] C. Zhu, G. Yang, H. Li, D. Du, Y. Lin, Anal. Chem. 87 (2015) 230-249.
[8] X. Chen, G. Wu, Z. Cai, M. Oyama, X. Chen, Microchim. Acta 181 (2013) 689-705.
[9] T. Chen, D. Liu, W. Lu, K. Wang, G. Du, A.M. Asiri, X. Sun, Anal. Chem. 88 (2016) 7885-7889.
[10] Y. Su, B. Luo, J.Z. Zhang, Anal. Chem. 88 (2016) 1617-1624.
[11] W. Zheng, L. Hu, L.Y.S. Lee, K.-Y. Wong, J. Electroanal. Chem. 781 (2016) 155-160.
[12] R. Ahmad, M. Vaseem, N. Tripathy, Y.-B. Hahn, Anal. Chem. 85 (2013) 10448-10454.
[13] C. Dong, H. Zhong, T. Kou, J. Frenzel, G. Eggeler, Z. Zhang, ACS Appl. Mater. Interfaces 7 (2015) 20215-20223.
[14] I. Shackery, U. Patil, A. Pezeshki, N.M. Shinde, S. Kang, S. Im, S.C. Jun, Electrochim. Acta 191 (2016) 954-961.
[15] J. Wang, D.F. Thomas, A. Chen, Anal. Chem. 80 (2008) 997-1004.

[16] Y. Song, X. Lu, Y. Li, Q. Guo, S. Chen, L. Mao, H. Hou, L. Wang, Anal. Chem. 88 (2016) 1371-1377.
[17] W. Zheng, Y. Li, M. Liu, C.-S. Tsang, L.Y.S. Lee, K.-Y. Wong, Electroanalysis 30 (2018) 1446-1454.
[18] M. Liu, R. Liu, W. Chen, Biosens. Bioelectron. 45 (2013) 206-212.
[19] D. Jiang, Q. Liu, K. Wang, J. Qian, X. Dong, Z. Yang, X. Du, B. Qiu, Biosens. Bioelectron. 54 (2014) 273-278.
[20] F. Huang, Y. Zhong, J. Chen, S. Li, Y. Li, F. Wang, S. Feng, Anal. Methods 5 (2013).
[21] K.E. Toghill, R.G. Compton, Int. J. Electrochem. Sci. 5 (2010) 1246-1301.
[22] W. Zhang, G. Jia, H. Li, S. Liu, C. Yuan, Y. Bai, D. Fu, J. Electrochem. Soc. 164 (2016) B40-B47.
[23] N. Gagnon, W.B. Tolman, Acc. Chem. Res. 48 (2015) 2126-2131.
[24] W. Zheng, Y. Li, C.-S. Tsang, L. Hu, M. Liu, B. Huang, L.Y.S. Lee, K.-Y. Wong, ChemElectroChem 4 (2017) 2788-2792.
[25] L.A. McDowell, H.L. Johnston, J. Am. Chem. Soc. 58 (1936) 2009-2014.
[26] Y. Deng, A.D. Handoko, Y. Du, S. Xi, B.S. Yeo, ACS Catal. 6 (2016) 2473-2481.
[27] X. Wang, C. Hu, H. Liu, G. Du, X. He, Y. Xi, Sens. Actuators, B 144 (2010) 220-225.
[28] E. Reitz, W. Jia, M. Gentile, Y. Wang, Y. Lei, Electroanalysis 20 (2008) 2482-2486.
[29] R.C. Alkire, P.N. Bartlett, J. Lipkowski, Electrochemistry of Carbon Electrodes, 2015, Wiley-VCH.
[30] K.-C. Lin, Y.-C. Lin, S.-M. Chen, Electrochim. Acta 96 (2013) 164-172.
[31] X. Zhang, G. Wang, W. Zhang, Y. Wei, B. Fang, Biosens. Bioelectron. 24 (2009) 3395-3398.
[32] Z. Sun, Z. Yang, J. Zhou, M.H. Yeung, W. Ni, H. Wu, J. Wang, Angew. Chem. Int. Ed. 48 (2009) 2881-2885.
[33] Y. Zhang, L. Su, D. Manuzzi, H.V. de los Monteros, W. Jia, D. Huo, C. Hou, Y. Lei, Biosens. Bioelectron. 31 (2012) 426-432.
[34] T. Yang, J. Xu, L. Lu, X. Zhu, Y. Gao, H. Xing, Y. Yu, W. Ding, Z. Liu, J. Electroanal. Chem. 761 (2016) 118-124.
[35] Y.-W. Hsu, T.-K. Hsu, C.-L. Sun, Y.-T. Nien, N.-W. Pu, M.-D. Ger, Electrochim. Acta 82 (2012) 152-157.
[36] N. Quoc Dung, D. Patil, H. Jung, D. Kim, Biosens. Bioelectron. 42 (2013) 280-286.
[37] S. Pourbeyram, K. Mehdizadeh, J. Food Drug Anal. 24 (2016) 894-902.
[38] V. Sharma, M. Chawla, J.K. Randhawa, J. Electrochem. Soc. 163 (2016) B594-B600.
[39] J. Bao, C. Hou, Y. Zhang, Q. Li, D. Huo, M. Yang, X. Luo, J. Electrochem. Soc. 162 (2014) B47-B51.
[40] M.E. Daly, C. Vale, M. Walker, A. Littlefield, K.G. Alberti, J.C. Mathers, Am. J. Clin. Nutr. 67 (1998) 1186-1196.
[41] Y.K. Kim, H. Park, Energy Environ. Sci. 4 (2011) 685-694.
[42] Z. Wang, Q. Zhang, D. Kuehner, X. Xu, A. Ivaska, L. Niu, Carbon 46 (2008) 1687-1692.
[43] T.I.T. Okpalugo, P. Papakonstantinou, H. Murphy, J. McLaughlin, N.M.D. Brown, Carbon 43 (2005) 153-161.

Conflict of Interest

The authors declare no conflict of interest.

Author contribution

Dr. W. Zheng and Y. Li conducted the electrochemical experiments and characterization. L. Hu helped with the discussion of experimental results. Dr. W. Zheng and Dr. L. Y. S. Lee drafted the manuscript together and Dr. L. Y. S. Lee supervised the project.

Acknowledge

We acknowledge the support from the Innovation and Technology Commission of Hong Kong and the Hong Kong Polytechnic University.

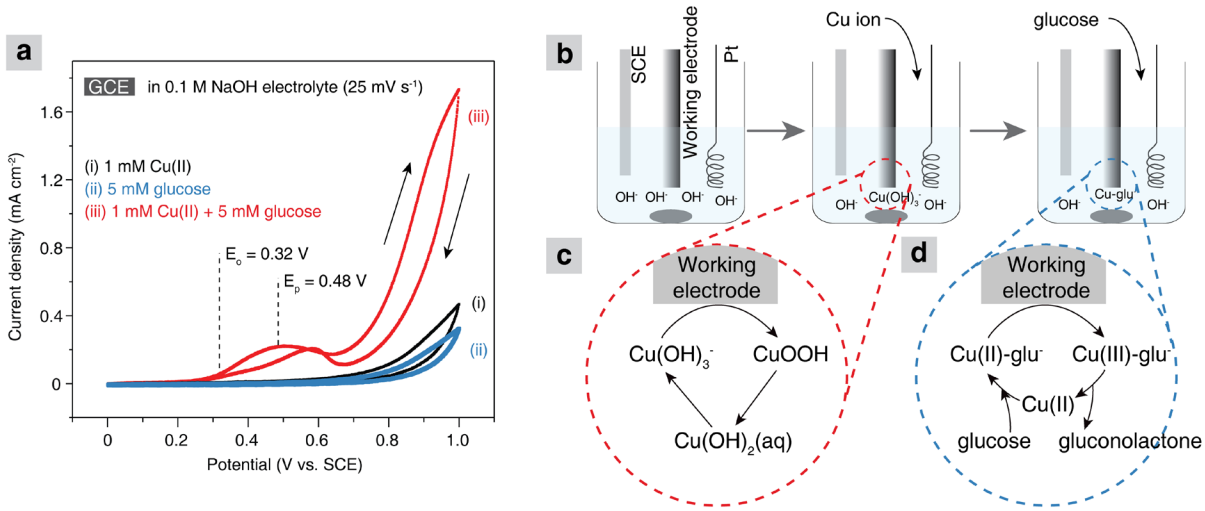

Figure 1. (a) CV plots of bare GCE in 0.1 M NaOH solution containing 1 mM Cu(II), 5 mM glucose, and 1 mM Cu(II) + 5 mM glucose. **(b)** Illustration of procedures of using Cu(II) for glucose sensing. **(c)** Reaction mechanism of bare GCE in an electrolyte containing only Cu(II). **(d)** Reaction mechanism of bare GCE in an electrolyte containing both Cu(II) and glucose.

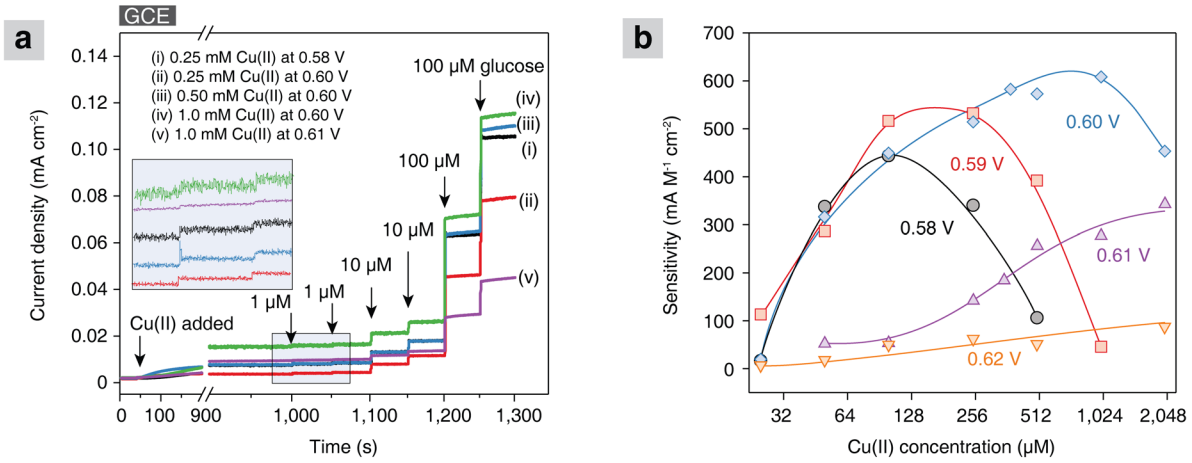

Figure 2. (a) Amperometric response of bare GCE with various Cu(II) concentrations at different potentials in 0.1 M NaOH. Cu(II) is added at 50s and glucose is added from 1,000s with concentration values labelled in the plot. **(b)** The sensitivity of glucose detection at different Cu(II) concentrations and different applied potentials using bare GCE.

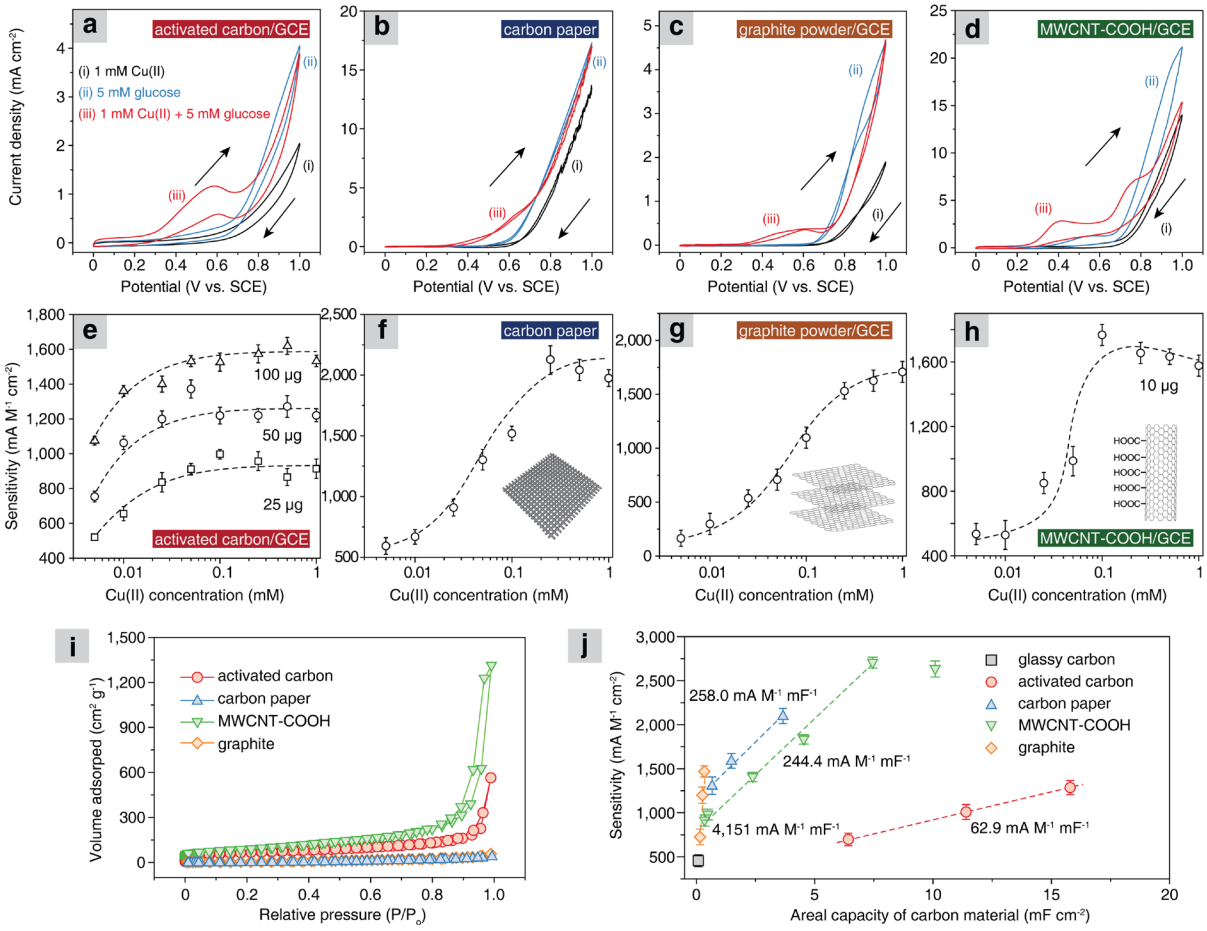

Figure 3. CV plots of carbon-based electrodes in 0.1 M NaOH solution containing 1 mM Cu(II), 5 mM glucose, and 1 mM Cu(II) + 5 mM glucose: **(a)** Nafion-activated carbon modified GCE; **(b)** carbon paper; **(c)** graphite powder modified GCE; **(d)** Nafion-MWCNT-COOH modified GCE, scan rate is 25 mV s^{-1}. Plots of the sensitivity of carbon-based electrodes towards glucose detection using different Cu(II) concentrations: **(e)** Nafion-activated carbon (25 µg, 50 µg, and 100 µg) modified GCE; **(f)** carbon paper (1 × 1 cm^2); **(g)** graphite powder (15 µg) modified GCE; **(h)** Nafion-MWCNT-COOH (10 µg) modified GCE. The insets are the structural illustration of used carbon-based electrodes. **(i)** The N_2 adsorption-desorption isotherms plots of carbon-based materials for BET surface area calculation. **(j)** Correlation between sensitivity towards glucose detection and areal capacity of carbon-based electrodes, Cu(II) ion concentration is 1 mM for all measurements. The inset values are the slopes of corresponding linear fit. Areal capacities are obtained by measuring the CV between 150 and 200 mV *vs.* SCE in 0.1 M NaOH.

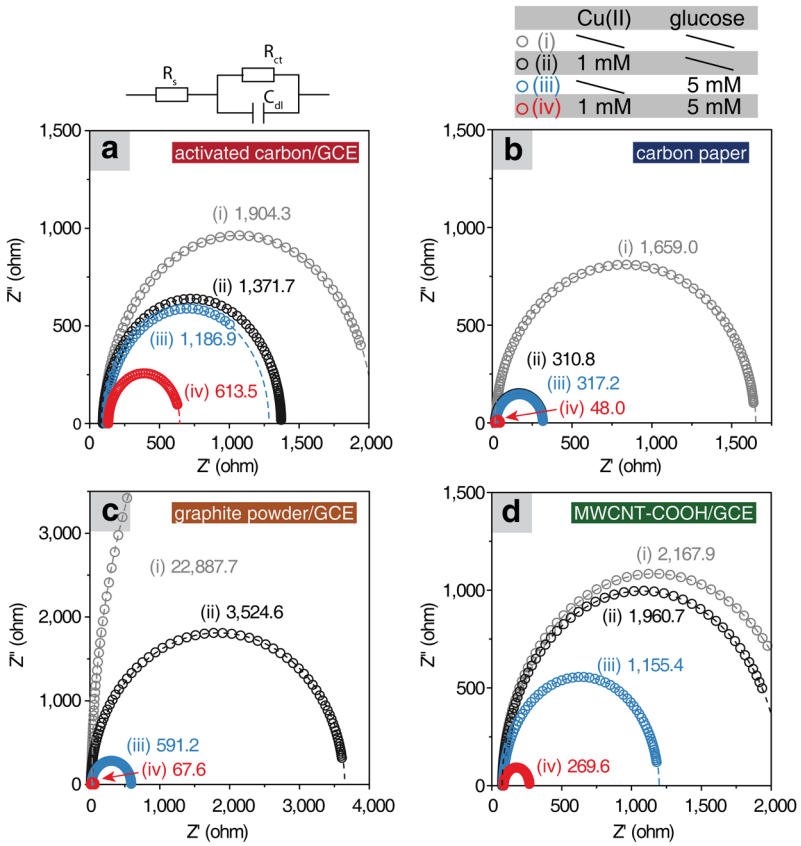

Figure 4. Nyquist plots of carbon-based electrodes at 0.60 V in 0.1 M NaOH containing different species (i. 0.1 M NaOH; ii. 0.1 M NaOH containing 1 mM Cu(II); iii. 0.1 M NaOH containing 5 mM glucose; and iv. 0.1 M NaOH containing 1 mM Cu(II) and 5 mM glucose) within 10 mHz to 1 M Hz. **(a)** Nafion-activated carbon (25 µg) modified GCE. **(b)** carbon fiber paper (1 × 1 cm^2). **(c)** graphite powder (15 µg)-modified GCE. **(d)** Nafion-MWCNT-COOH (10 µg)-modified GCE. All EIS results are fitted with a simplified Randles cell as shown above (a), and the fitted resistance values (R_{ct}) are shown in the plots.

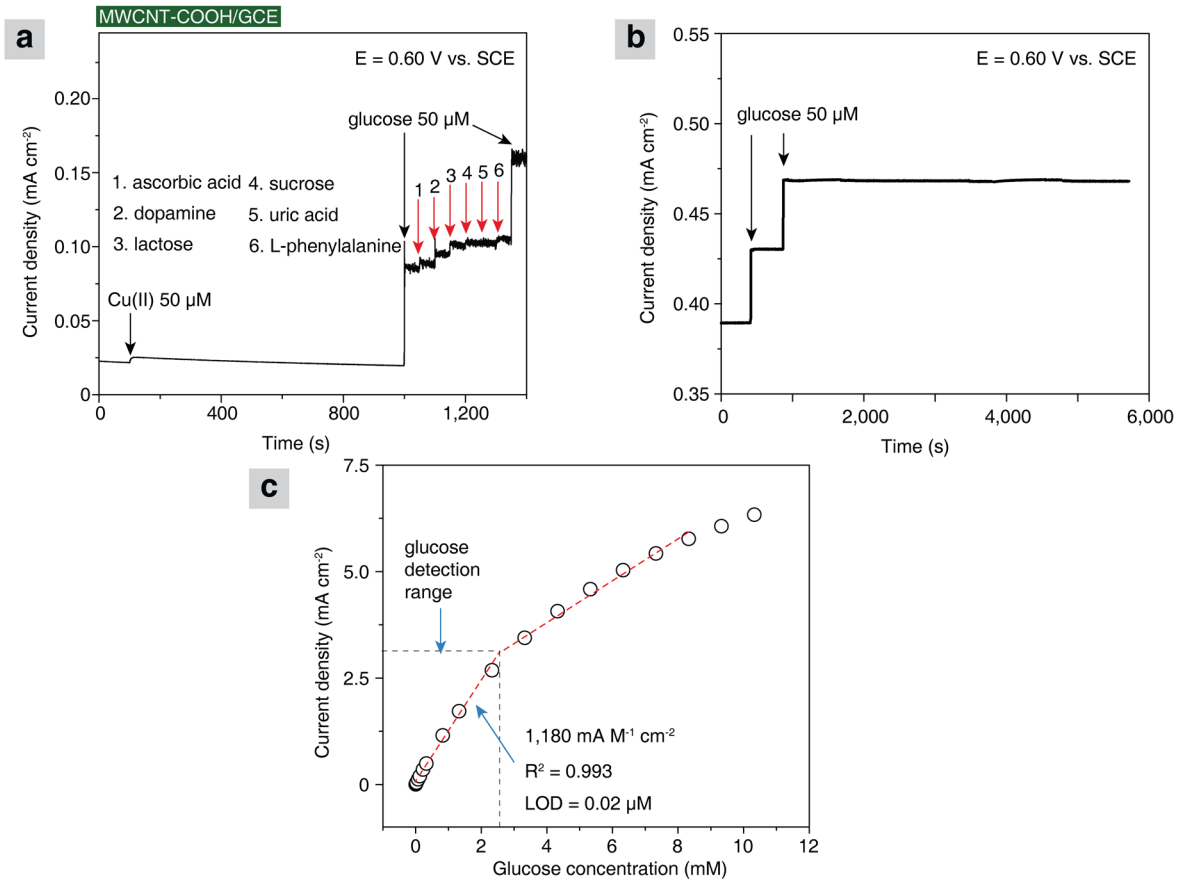

Figure 5. (a) Interference test using a MWCNT-COOH (10 µg) modified GCE at an applied potential of 0.60 V with 0.05 mM Cu(II) in electrolyte. 5 µM interferents were added at times indicated with arrows. **(b)** Stability test at 0.60 V using MWCNT-COOH (10 µg) modified GCE with 0.05 mM Cu(II). **(c)** Correlation between glucose concentration and current density using a MWCNT-COOH (10 µg) modified GCE with 0.05 mM Cu(II) for glucose sensing. The slope value in the glucose concentration range between 0 and 2.5 mM is shown.

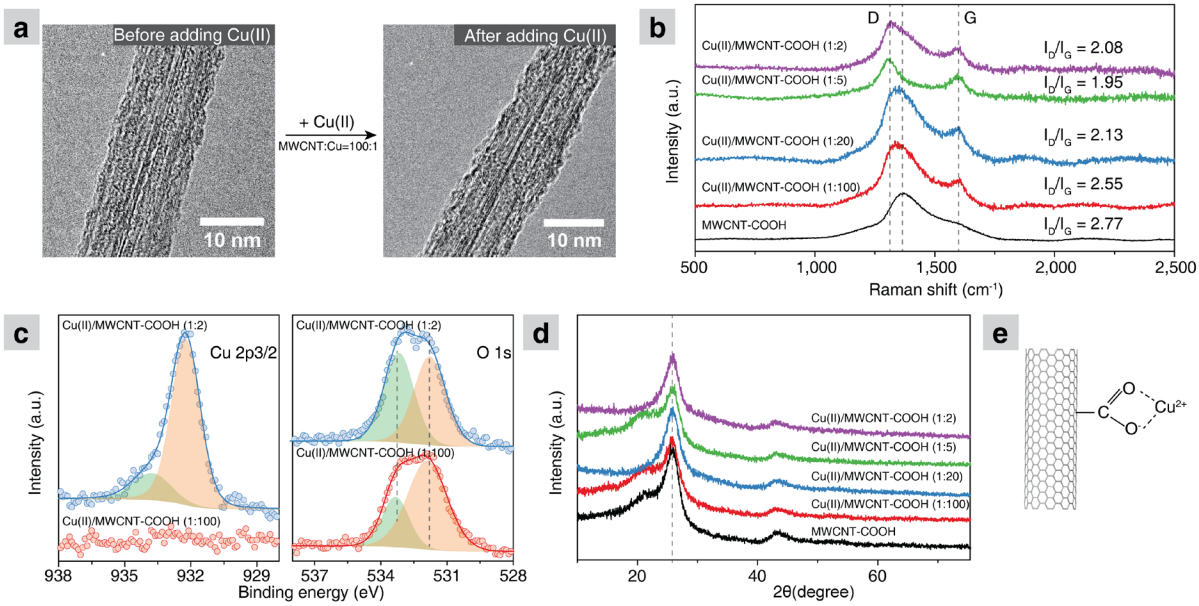

Figure 6. (a) TEM images MWCNT-COOH before and after introducing Cu(II). **(b)** Raman spectra of MWCNT-COOH and Cu(II)/MWCNT-COOH; **(c)** XPS spectra of Cu $2p_{3/2}$ and O 1s region of Cu(II)/MWCNT-COOH (1:100) and Cu(II)/MWCNT-COOH (1:2). **(d)** XRD plots of MWCNT-COOH and Cu(II)/MWCNT-COOH; **(e)** Illustration of possible structure of Cu(II)/MWCNT-COOH.

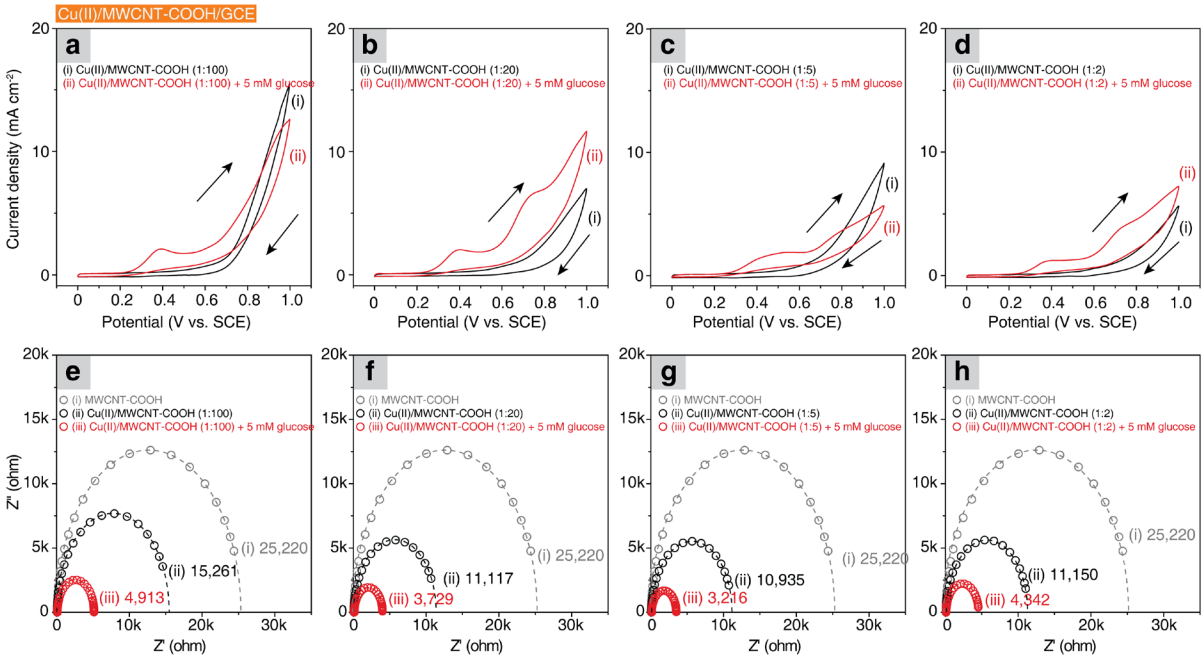

Figure 7. CV plots of Cu(II)/MWCNT-COOH modified GCE in 0.1 M NaOH solution with and without 5 mM glucose: **(a)** Cu(II)/MWCNT-COOH = 1:100; **(b)** Cu(II)/MWCNT-COOH = 1:20; **(c)** Cu(II)/MWCNT-COOH = 1:5; **(d)** Cu(II)/MWCNT-COOH = 1:2. Scan rate is 25 mV s^{-1}. Nyquist plots of Cu(II)/MWCNT-COOH modified GCE at 0.60 V in 0.1 M NaOH solution with and without 5 mM glucose, the plot of MWCNT-COOH modified GCE is presented for comparison: **(e)** Cu(II)/MWCNT-COOH = 1:100; **(f)** Cu(II)/MWCNT-COOH = 1:20; **(g)** Cu(II)/MWCNT-COOH = 1:5; **(h)** Cu(II)/MWCNT-COOH = 1:2. All EIS results are fitted with a simplified Randles cell as shown in Figure 4, and the fitted resistance values (R_{ct}) are shown in the plots.

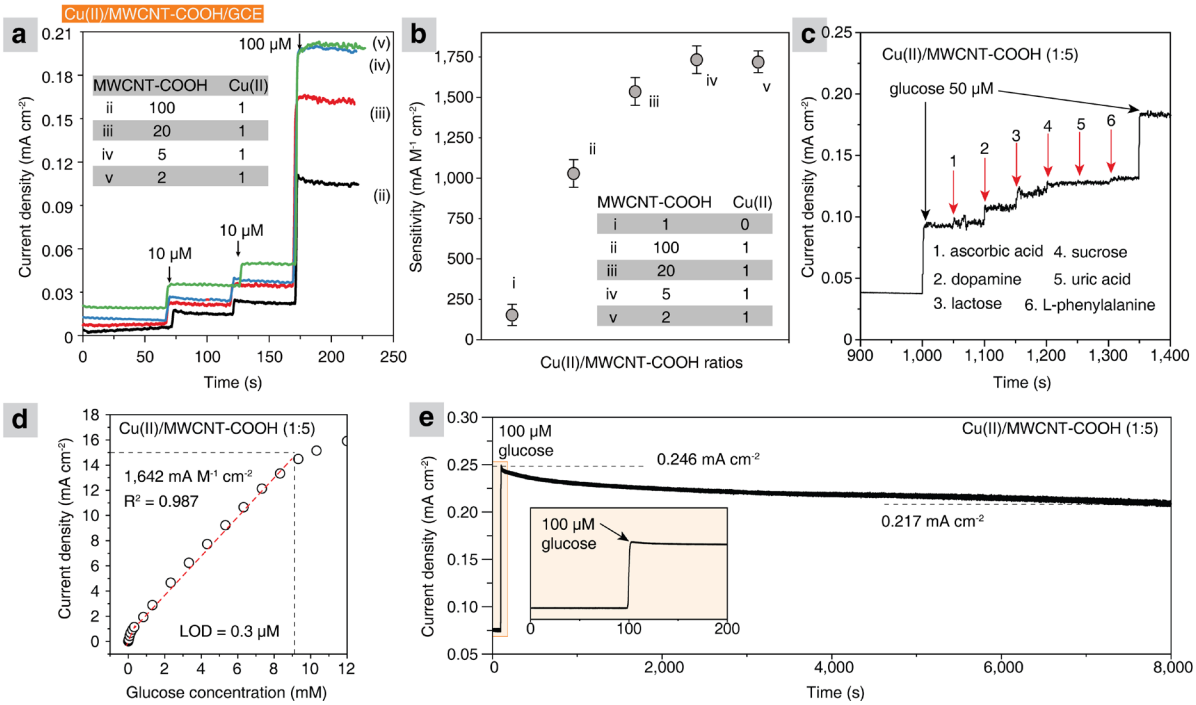

Figure 8. (a) Amperometric response of Cu(II)/MWCNT-COOH modified GCE (mass ratio of Cu^{II} to MWCNT-COOH varies from 1:100 to 1:2 , and the weight of MWCNT-COOH is fixed at 10 µg) to glucose addition. **(b)** Summary of sensitivity values obtained from MWCNT-COOH and Cu(II)/MWCNT-COOH modified GCE. **(c)** Interference test using Cu(II)/MWCNT-COOH modified GCE (1:5) at an applied potential of 0.60 V. 5 µM interferents were introduced at times indicated with arrows. **(d)** Correlation between glucose concentration and current density using a Cu(II)/MWCNT-COOH (1:5) modified GCE for glucose sensing. The slope value in the glucose concentration range between 0.3 and 9.0 mM is shown. **(e)** Stability test at 0.60 V using Cu(II)/MWCNT-COOH (1:5) modified GCE for glucose electrooxidation.